



Modelling and Simulation of Bearing Clearance Effects on the Chatter Stability of Turning Process

Sebastian Oaihimire Amiebenomo¹, Chigbogu G. Ozoegwu^{2*} and Osagie Ighodalo¹

¹Department of Mechanical Engineering, Ambrose Alli University, Ekpoma, Nigeria

²Department of Mechanical Engineering, University of Nigeria, Nsukka, Nigeria

*Corresponding author E-mail address: amiebenomosebastian@aauekpoma.edu.ng

ABSTRACT

There is a paucity of theoretical studies on the bearing clearance of the motor drive unit of the lathe and its impact on chatter stability during turning of machined parts. This study considers theoretically the development of an analytical model to establish the influence of bearing clearance (BC) on regenerative chatter vibration in a turning process. In the course of this work, analytical model of the bearing clearance variable was developed. The analytical solution of the developed model was generated using Time Domain Simulation (TDS) to establish the effect of bearing clearance on the regenerative chatter stability of the turning process. The simulations entail the use of cylindrical roller bearings of nominal bore diameter of 50 mm with bearing clearance values of 60×10^{-6} m, 80×10^{-6} m and 110×10^{-6} m at two spindle speeds of 10000rpm and, 3000rpm, and depths of cut of 0.5mm and 1mm respectively. The results of simulations employing the time histories of displacement and velocity and phase plots showed chatter instability associated with bearing clearance as indicated by the divergence with time from an attractor.

Key words: Bearing clearance, Time-domain simulation, Time histories, Displacement history, Velocity history, Phase plots, Turning process

INTRODUCTION

Metal cutting is a complex nonlinear dynamical process [1]. The machine, the cutting tool and the workpiece form a complex system which has infinite number of degrees of freedom. The cutting process under dynamic conditions can behave in different ways for different modes of vibration [2]. It is therefore noted that one of the main challenges, as it effects the surface roughness of machined parts, imparts on tool life and results in noise during machining operations, is unwanted vibration in conventional machine tools such as the lathe [3].

Bearings are one of the most common among machine elements and very significant in all forms of rotating machinery. Bearings are designed to provide a very significant level of rotational accuracy and rigidity, while offering material cost saving and space conservation [4]. The cutting performance of bearings are affected by manufacturing setting accuracy and installation [4]. During bearing installation, manufacturer guidelines are strictly followed. Test are usually done after installation to evaluate the spindle bearing cutting performance. Additionally, the quality of finished parts is affected by tool geometry, cutting parameters and vibration.

There are many published studies on machine tool spindle bearing unit in terms of modelling their performance and bearing condition analysis as pertain to varied forms of vibration imparts on them. Yuzhong, and Altintas, [5] developed a combine model of a spindle bearing and machine tool system. The system model was made up of rotating shaft, tool holder, angular ball bearing, housing and machine mounting. The developed model was deployed for predicting the stiffness of bearing mode shapes, frequency response function (FRF), cutter and spindle deflection (static and dynamic) and bearing contact forces. The experimental validation of the model reveals that negative bearing clearance, cutting parameters and the properties of the workpiece employed affect the frequency and amplitude of vibration in the course of machining. The significance of interference fit on static and dynamic properties of a spindle system was investigated by Liu, Hong, Wenwu, and Sun, [6]. An analytical spindle bearing model was proposed and the results of analysis obtained show that interference fits lead to increase stiffness of the

bearing and spindle system at higher values of natural frequencies. Analytical model accuracy was found to be 7.86%.

Since the 1980s, new concepts of modelling, measuring, and controlling nonlinear dynamics in cutting processing have appeared. Various nonlinear effects on cutting dynamics include tool structure nonlinearities, friction at the tool-chip interface, loss of tool-workpiece contact, material constitutive relations (stress versus strain, strain rate, and temperature) and influence of machine drive unit on the cutting flow velocity. Most research efforts have usually been made to investigate the first four kinds of nonlinear effects [7-11]. A common fault or defect associated with the machine drive unit of lathe is the bearing clearance. The internal clearance of a bearing under operating conditions (effective clearance) is usually smaller than the same bearing's initial clearance before being installed and operated. A number of factors are responsible such as bearing fit; temperature differential between inner and outer rings. Given that the operating clearance in bearing has an influence on bearing life, heat generation and vibration, it becomes imperative that detail consideration be given in the selection of an appropriate operating clearance [12]. Machine tool dynamics has been an important issue due to its significant role in the chatter stability and other outcomes of the process. In predicting instability, reliable results are only obtained when the dynamics of the structure and cutting process are correctly incorporated in the analysis.

Researchers have examined bearing clearance effects in the modelling of chatter vibrations in a milling process, see [13], but there is a dearth of information which establishes its effect on chatter stability of turning process. Theoretical assessment of the effects of bearing clearance on the chatter stability of turning process is therefore the thrust of this work.

METHODOLOGY

A Multibody Model of Turning Regenerative Chatter

In this section, the analytical procedures for investigating turning regenerative chatter without bearing clearance and subsequently with bearing clearance are outline.

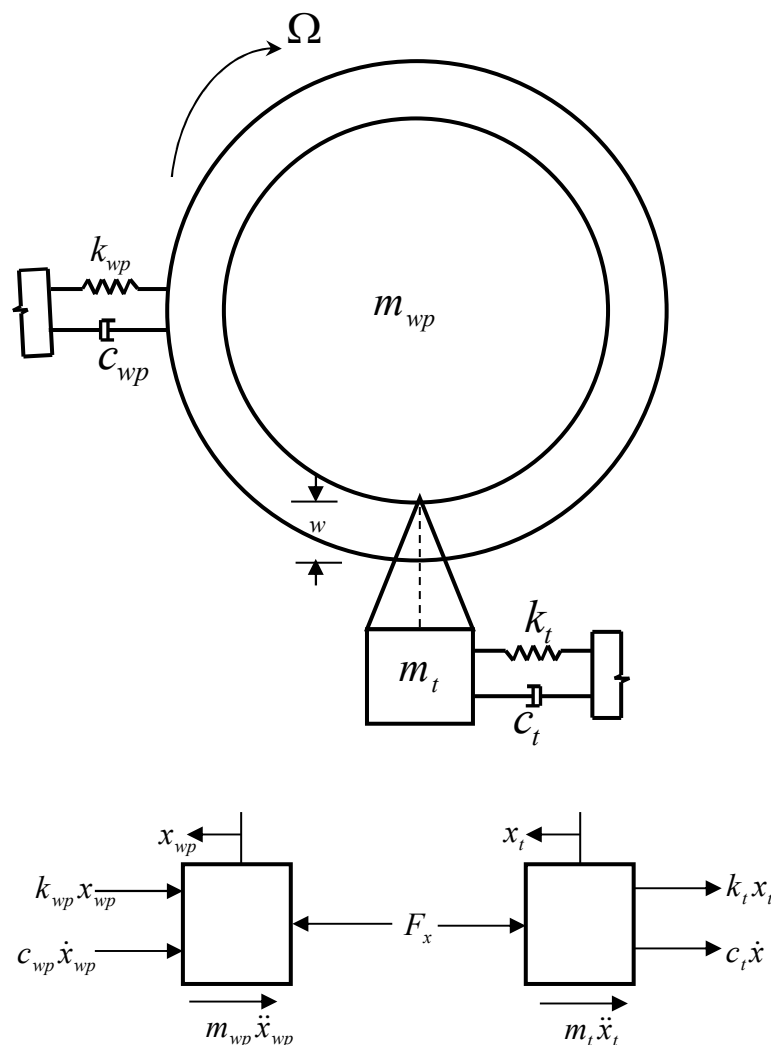


Fig. 1 The 2DOF multibody mechanical model of turning and its free-body diagram

The lathe spindle is supported on the bearings; therefore, the conditions of the bearings directly affect the spindle dynamics. In turning process, the workpiece is clamped via chucks to the spindle thus the bearing effects are relayed to the workpiece through the spindle. Therefore, the workpiece-spindle system must be considered system compliant for the bearing effects to be studied. This suggests multibody model of turning regenerative chatter as the applicable model and efforts should evolve from such advanced model without clearance effects. For the 2DOF multibody system without bearing clearance, the mechanical model and its free-body diagram are indicated in Figure 1.

The contact between the tool and the workpiece evokes the Newton's third law; action and reaction are equal and opposite, which is obeyed in the free-body diagram. The cutting process in the tangential (or feed-normal) cutting direction "x" is considered. The feed direction "y" is into the page and the regenerative vibration in that direction is not as important in the study of bearing effect on regenerative turning. In the model, the quantities subscripted with "wp" indicate modal parameters of the workpiece-spindle system while those quantities subscripted with "t" indicate modal parameters of the tool system. From the free-body diagram, it can be seen that

$$m_t \ddot{x}_t(t) + c_t \dot{x}_t(t) + k_t x_t(t) + F_x(t) = 0, \quad (1a)$$

$$m_{wp} \ddot{x}_{wp}(t) + c_{wp} \dot{x}_{wp}(t) + k_{wp} x_{wp}(t) - F_x(t) = 0. \quad (1b)$$

Regenerative effects are usually quantified as fluctuations of the tool cutting edge about the prescribed undeformed chip thickness. When the tool is considered a compliant system in contact with a compliant workpiece-spindle system then the regenerative effects become quantified as the fluctuations of the relative motion between the two contacting bodies about the undeformed chip thickness. Therefore, the force $F_x(t)$ is the linear cutting force model in the feed-normal direction given as [14].

$$F_x(t) = Cw[x_t(t) - x_{wp}(t) - x_t(t - \tau) + x_{wp}(t - \tau)] \quad (2)$$

Inserting Equation (2) in Equation (1) gives

$$m_t \ddot{x}_t(t) + c_t \dot{x}_t(t) + (k_t + Cw)x_t(t) - Cw x_t(t - \tau) - Cw[x_{wp}(t) - x_{wp}(t - \tau)] = 0, \quad (3a)$$

$$m_{wp} \ddot{x}_{wp}(t) + c_{wp} \dot{x}_{wp}(t) + (k_{wp} + Cw)x_{wp}(t) - Cw x_{wp}(t - \tau) - Cw[x_t(t) - x_t(t - \tau)] = 0. \quad (3b)$$

The modal form of Equation (3) becomes

$$\ddot{x}_t(t) + 2\zeta_t \omega_{nt} \dot{x}_t(t) + \left(\omega_{nt}^2 + \frac{Cw}{m_t}\right) x_t(t) - \frac{Cw}{m_t} x_{wp}(t) = \frac{Cw}{m_t} x_t(t - \tau) - \frac{Cw}{m_t} x_{wp}(t - \tau), \quad (4a)$$

$$\ddot{x}_{wp}(t) + 2\zeta_{wp} \omega_{nwp} \dot{x}_{wp}(t) + \left(\omega_{nwp}^2 + \frac{Cw}{m_{twp}}\right) x_{wp}(t) - \frac{Cw}{m_{twp}} x_t(t) = \frac{Cw}{m_{twp}} x_{wp}(t - \tau) - \frac{Cw}{m_{twp}} x_t(t - \tau). \quad (4b)$$

Let $x_1 = x_t(t)$, $x_2 = \dot{x}_t(t)$, $x_3 = x_{wp}(t)$ and $x_4 = \dot{x}_{wp}(t)$ then the first-order form is constructed and represented in compact form as

$$\dot{\mathbf{x}} = \mathbf{A}\mathbf{x} + \mathbf{B}\mathbf{x}(t - \tau), \quad (5)$$

where

$$\mathbf{A} = \begin{bmatrix} 0 & 1 & 0 & 0 \\ -\left(\omega_{nt}^2 + \frac{Cw}{m_t}\right) & -2\zeta_t \omega_{nt} & \frac{Cw}{m_t} & 0 \\ 0 & 0 & 0 & 1 \\ \frac{Cw}{m_{twp}} & 0 & -\left(\omega_{nwp}^2 + \frac{Cw}{m_{twp}}\right) & -2\zeta_{wp} \omega_{nwp} \end{bmatrix} \quad (6)$$

$$\mathbf{B} = \begin{bmatrix} 0 & 0 & 0 & 0 \\ \frac{Cw}{m_t} & 0 & -\frac{Cw}{m_t} & 0 \\ 0 & 0 & 0 & 0 \\ -\frac{Cw}{m_{twp}} & 0 & \frac{Cw}{m_{twp}} & 0 \end{bmatrix} \quad (7)$$

A multibody model of turning regenerative chatter considering clearance effects is considered next before simulation and analysis of the nature of the effects.

The Development of Turning Regenerative Chatter Considering Bearing Clearance Effect

The bearing clearance effect finally gets to the tool via the cutting interaction between the tool and the workpiece. As already discussed in literature [8, 13, 15], bearing clearance effects are captured as a form of discontinuous stiffness. This is illustrated in Figure 2 for the cutting direction. The governing equation of motion becomes

$$m_t \ddot{x}_t(t) + c_t \dot{x}_t(t) + k_t x_t(t) + F_x(t) = 0, \tag{8a}$$

$$m_{wp} \ddot{x}_{wp}(t) + c_{wp} \dot{x}_{wp}(t) + k_{wp} x_{wp}(t) + \delta(x_{wp} - \gamma) k_{bc} [x_{wp} - \gamma] - F_x(t) = 0, \tag{8b}$$

where k_{bc} is the equivalent stiffness modelling bearing clearance, $\delta(x_{wp} - \gamma)$ is a screening function defined as

$$\delta(x_{wp} - \gamma) = 1 \text{ if } x_{wp} - \gamma \geq 0, \tag{9a}$$

$$\delta(x_{wp} - \gamma) = 0 \text{ if } x_{wp} - \gamma < 0, \tag{9b}$$

and γ is the bearing clearance. With the designation $\Delta = x_{wp} - \gamma$, Equation (8) becomes re-arranged as

$$m_t \ddot{x}_t(t) + c_t \dot{x}_t(t) + k_t x_t(t) + F_x(t) = 0, \tag{10a}$$

$$m_{wp} \ddot{x}_{wp}(t) + c_{wp} \dot{x}_{wp}(t) + [k_{wp} + \delta(\Delta) k_{bc}] x_{wp}(t) - [\delta(\Delta) k_{bc} \gamma + F_x(t)] = 0. \tag{10b}$$

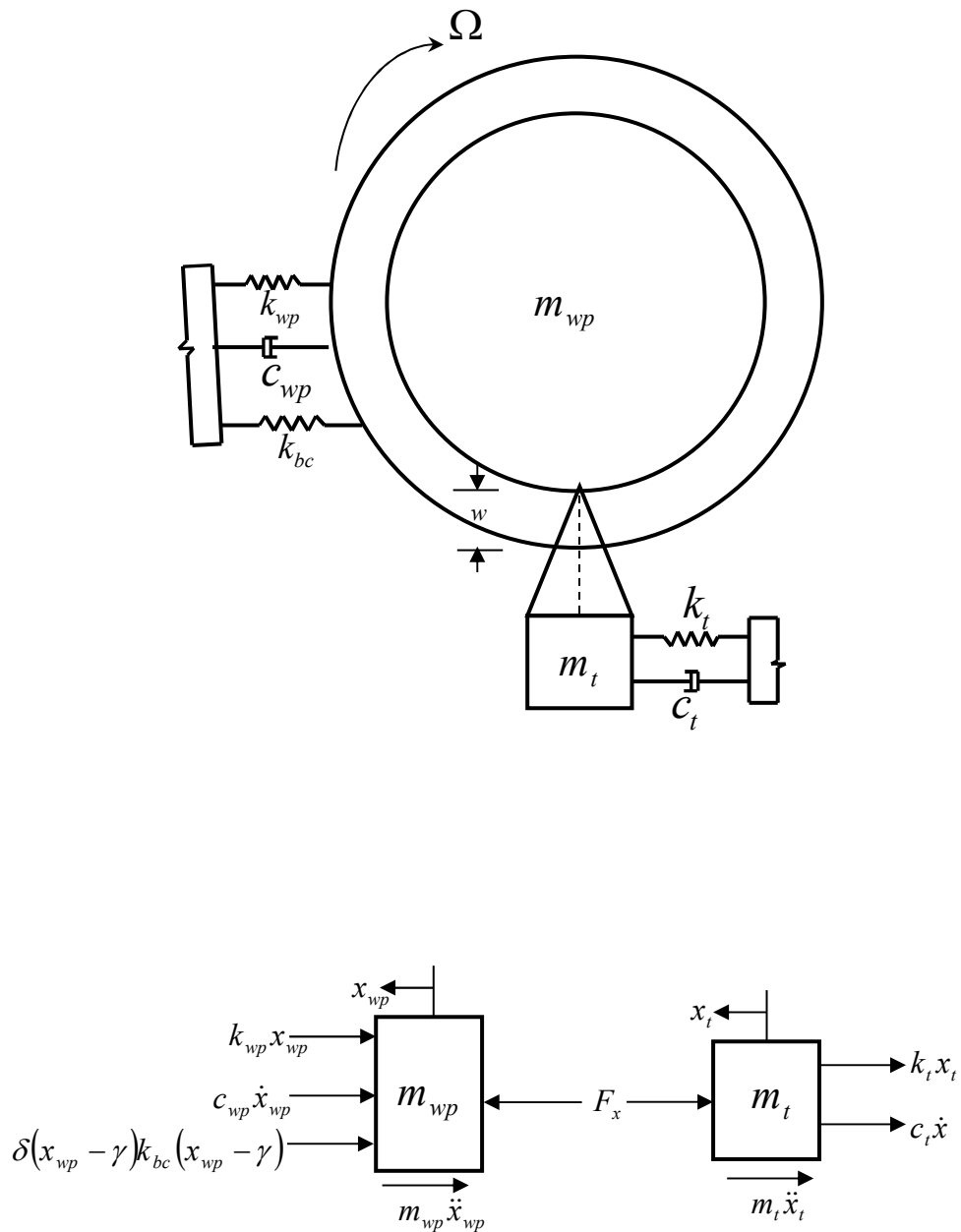


Fig. 2 The 2DOF multibody mechanical model of turning with bearing clearance effect and its free-body diagram

The force $F_x(t)$ is as given in Equation (2). Therefore, inserting $F_x(t)$ in Equation (10) gives

$$m_t \ddot{x}_t(t) + c_t \dot{x}_t(t) + (k_t + Cw)x_t(t) - Cw x_t(t - \tau) - Cw[x_{wp}(t) - x_{wp}(t - \tau)] = 0, \quad (11a)$$

$$m_{wp} \ddot{x}_{wp}(t) + c_{wp} \dot{x}_{wp}(t) + (k_{wp} + \delta(\Delta)k_{bc} + Cw)x_{wp}(t) - Cw x_{wp}(t - \tau) - Cw[x_t(t) - x_t(t - \tau)] - \delta(\Delta)k_{bc}\gamma = 0. \quad (11b)$$

The modal form becomes

$$\ddot{x}_t(t) + 2\zeta_t \omega_{nt} \dot{x}_t(t) + \left(\omega_{nt}^2 + \frac{Cw}{m_t}\right)x_t(t) - \frac{Cw}{m_t}x_{wp}(t) = \frac{Cw}{m_t}x_t(t - \tau) - \frac{Cw}{m_t}x_{wp}(t - \tau), \quad (12a)$$

$$\ddot{x}_{wp}(t) + 2\zeta_{wp} \omega_{nwp} \dot{x}_{wp}(t) + \left(\omega_{nwp}^2 + \frac{\delta(\Delta)k_{bc}}{m_{twp}} + \frac{Cw}{m_{twp}}\right)x_{wp}(t) - \frac{Cw}{m_{twp}}x_t(t) = \frac{Cw}{m_{twp}}x_{wp}(t - \tau) - \frac{Cw}{m_{twp}}x_t(t - \tau) + \frac{\delta(\Delta)k_{bc}}{m_{twp}}\gamma. \quad (12b)$$

Let $x_1 = x_t(t)$, $x_2 = \dot{x}_t(t)$, $x_3 = x_{wp}(t)$ and $x_4 = \dot{x}_{wp}(t)$, then the first order form is constructed and put in the matrix form as

$$\dot{\mathbf{x}} = \mathbf{A}\mathbf{x} + \mathbf{B}\mathbf{x}(t - \tau) + \mathbf{d}, \quad (13)$$

where

$$\mathbf{A} = \begin{bmatrix} 0 & 1 & 0 & 0 \\ -\left(\omega_{nt}^2 + \frac{Cw}{m_t}\right) & -2\zeta_t \omega_{nt} & \frac{Cw}{m_t} & 0 \\ 0 & 0 & 0 & 1 \\ \frac{Cw}{m_{twp}} & 0 & -\left(\omega_{nwp}^2 + \frac{\delta(\Delta)k_{bc}}{m_{twp}} + \frac{Cw}{m_{twp}}\right) & -2\zeta_{wp} \omega_{nwp} \end{bmatrix}, \quad (14)$$

$$\mathbf{B} = \begin{bmatrix} 0 & 0 & 0 & 0 \\ \frac{Cw}{m_t} & 0 & -\frac{Cw}{m_t} & 0 \\ 0 & 0 & 0 & 0 \\ -\frac{Cw}{m_{twp}} & 0 & \frac{Cw}{m_{twp}} & 0 \end{bmatrix}, \quad (15)$$

$$\mathbf{d} = \begin{bmatrix} 0 \\ 0 \\ 0 \\ \frac{\delta(\Delta)k_{bc}}{m_{twp}}\gamma \end{bmatrix}. \quad (16)$$

It is impossible for the current form of the developed model and at the current level of development to generate pure analytical solution of the model with bearing clearance; therefore, its stability analyses cannot result in close form expressions. The method that is applicable to this form of differential equation is the method of time domain simulation (TDS) and it is adopted here.

SIMULATION

The effect of bearing clearance on turning chatter stability is investigated in what follows. The bearing clearance values for cylindrical roller bearings of nominal bore diameter of 50 mm used for simulations are 60×10^{-6} m, 80×10^{-6} m and 110×10^{-6} m. For purpose of model validity, experimental bearing clearance of 5×10^{-6} m used in Peng et al (2010) was employed for simulation. An equivalent bearing clearance stiffness of $k_{bc} = 0.5k_{wp} = 0.5m_{wp}\omega_{nwp}^2$ is adopted. The history is as follows; $y_1(t \leq 0) = f/1000 = v\tau/1000$, $y_2(t \leq 0) = v$, $y_3(t \leq 0) = f/1000 = v\tau/1000$ and $y_4(t \leq 0) = v$ where $v = 0.0025 \text{ ms}^{-1}$. As adopted from Fisher and Eberhard (2014), the modal parameters used for simulation are summarized in Table 1 while the cutting force coefficient is $C = 3.5 \times 10^9 \text{ N/m}$.

Table -1 Modal Parameters of Multibody Turning

Tool	$m_t = 50\text{g}$	$\omega_{nt} = 775\text{rad/s}$	$\zeta_t = 0.05$
Workpiece	$m_{wp} = 50\text{g}$	$\omega_{nwp} = 650\text{rad/s}$	$\zeta_{wp} = 0.05$

Simulation of Bearing Clearance Effect on Regenerative Chatter of Turning Process

The simulations for the case of no bearing clearance and bearing clearance of 60×10^{-6} m are juxtaposed in Tables 2 to 4 for direct comparison. More simulations are given in Figs 3 to 5 for the bearing clearance values of $80 \times$

$10^{-6}m, 110 \times 10^{-6}m$ and $5 \times 10^{-6}m$. The simulations are presented in the forms: time histories and phase portraits.

Table -2 Velocity history

Ω [rpm]	W [mm]	Without BC	With BC of $60 \times 10^{-6}m$
3000	0.5		
1000	0		
3000	1		
1000	1		

Table -3 Displacement history

Ω [rpm]	W [mm]	Without BC	With BC of 60×10^{-6} m
3000	0.5		
1000	0		
3000	1		
1000	1		

Table -4 Phase trajectories

Ω [rpm]	W [mm]	Without BC	With BC of 6×10^{-6} m
3000	0.5		
10000	0.5		
3000	1		
10000	1		

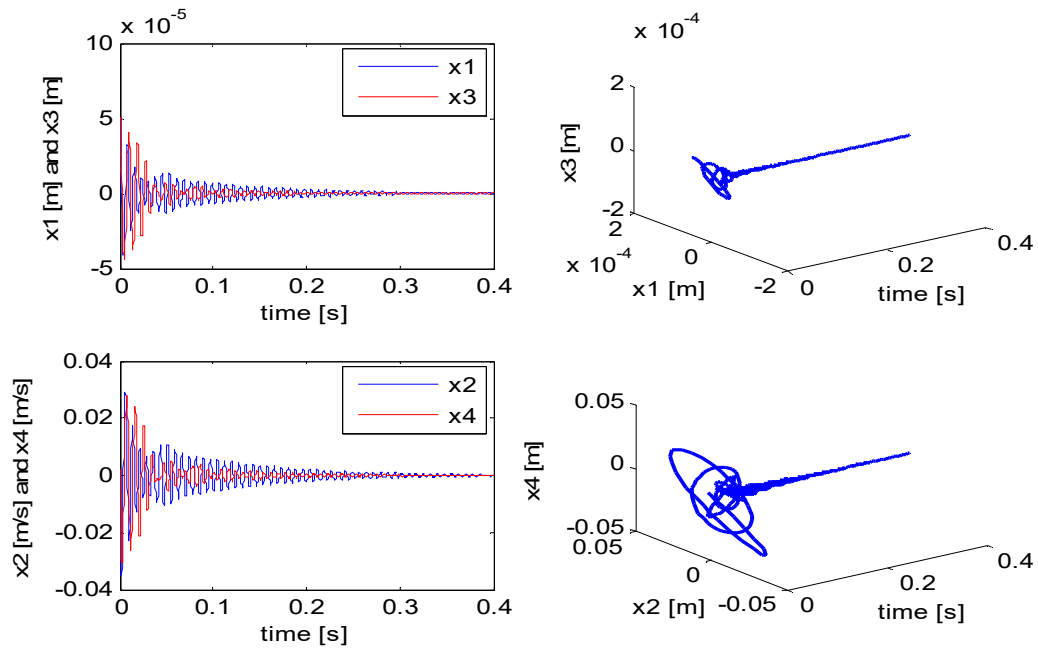


Fig. 3 The time histories of multibody turning model without BC when $\Omega=3000\text{rpm}$ and $w=0.5\text{mm}$. (The first column contains the plane plot which has two equivalent responses of the tool and the workpiece on vertical axis. The second column is the equivalent 3D line plots.)

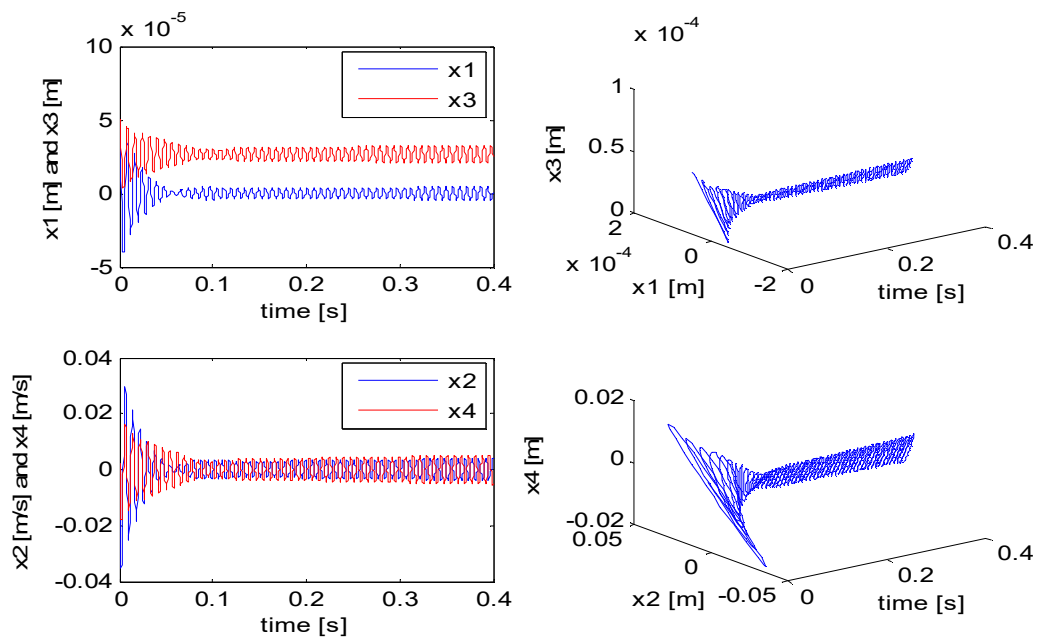


Fig. 4 The time histories of multibody turning model with $BC=80 \times 10^{-6}\text{m}$ when $\Omega=3000\text{rpm}$ and $w=0.5\text{mm}$. (The first column contains the plane plot which has two equivalent responses of the tool and the workpiece on the vertical axis. The second column contains the equivalent 3D line plots.)

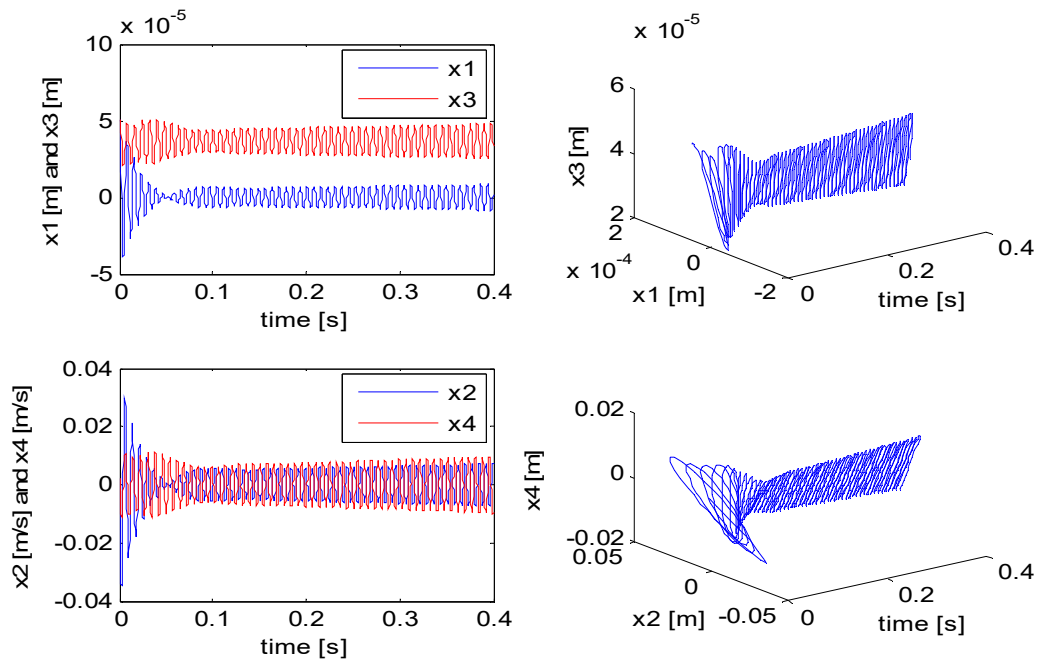


Fig. 5 The time histories of multibody turning model with $BC=110 \times 10^{-6}m$ when $\Omega=3000rpm$ and $w=0.5mm$. (The first column contains the plane plot which has two equivalent responses of the tool and the workpiece on the vertical axis. The second column contains the equivalent 3D line plots.)

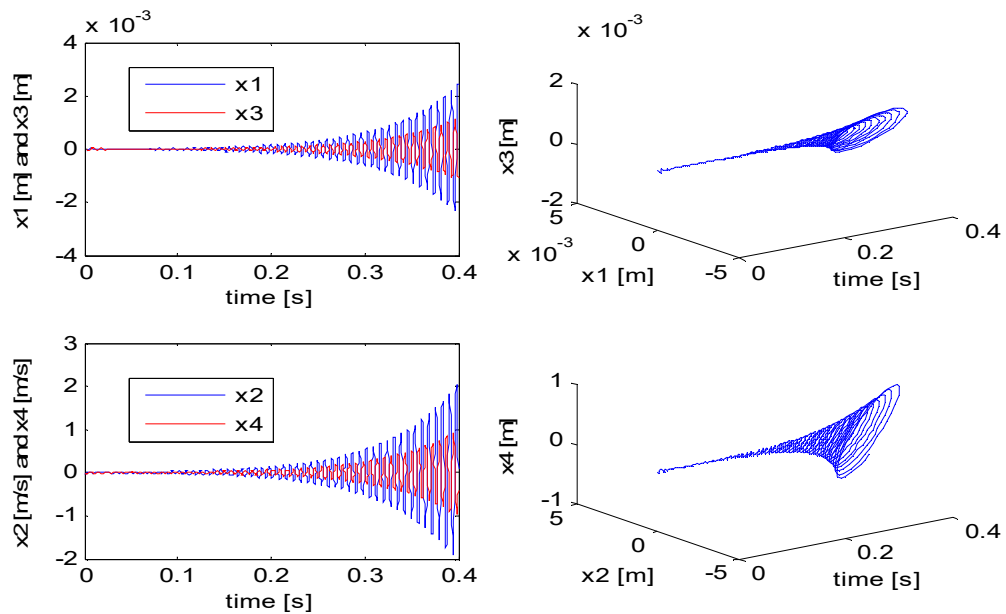


Fig. 6 The time histories of multibody turning model without BC when $\Omega=3000rpm$ and $w=1mm$. (The first column contains the plane plot which has two equivalent responses of the tool and the workpiece on the vertical axis. The second column contains the equivalent 3D line plots. The turning process is unstable.)

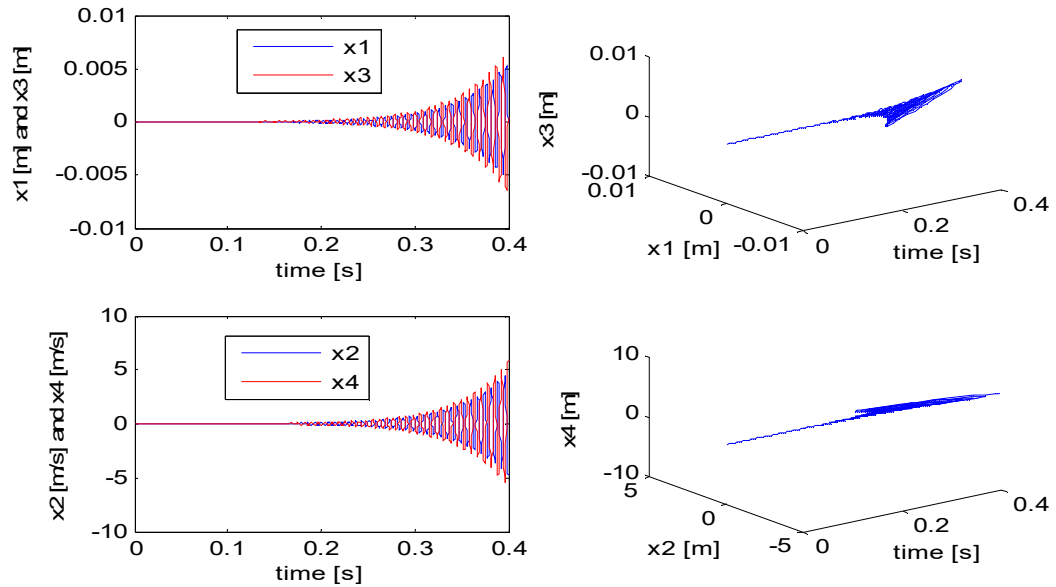


Fig. 7 The time histories of multibody turning model with $BC=80 \times 10^{-6}m$ when $\Omega=3000rpm$ and $w=1mm$. (The first column contains the plane plot which has two equivalent responses of the tool and the workpiece on the vertical axis. The second column contains the equivalent 3D line plots. The turning process is unstable.)

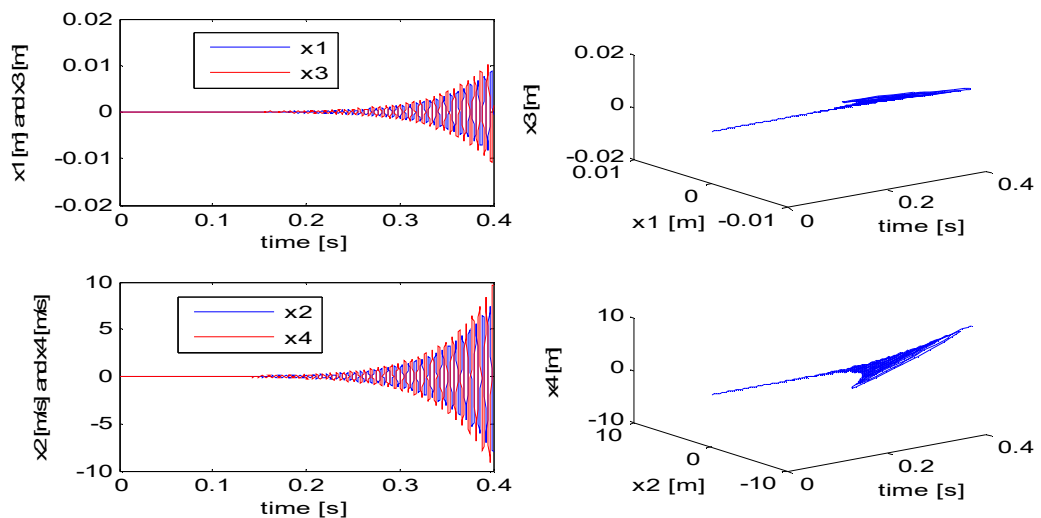


Fig. 8 The time histories of multibody turning model with $BC=110 \times 10^{-6}m$ when $\Omega=3000rpm$ and $w=1mm$. (The first column contains the plane plot which has two equivalent responses of the tool and the workpiece on the vertical axis. The second column contains the equivalent 3D line plots. The turning process is unstable.)

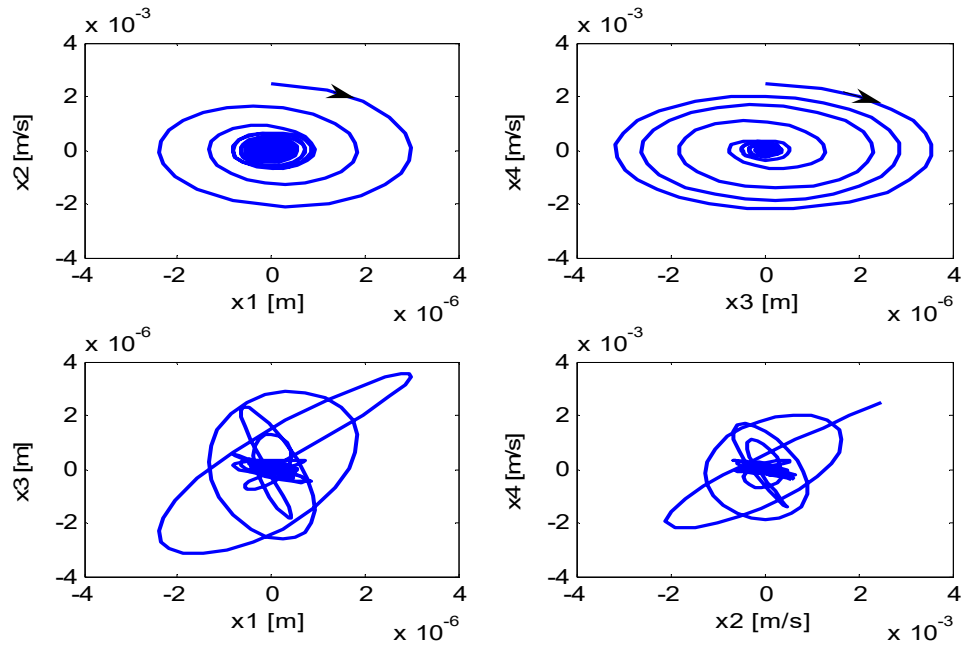


Fig. 9 The Phase plots of multibody turning model without BC when $\Omega=3000\text{rpm}$ and $w=0.5\text{mm}$. (The first row contains the phase plots of the tool and the workpiece respectively while the second row contains the plots of displacements which is a measure of cutting zone location. Stability is seen.)

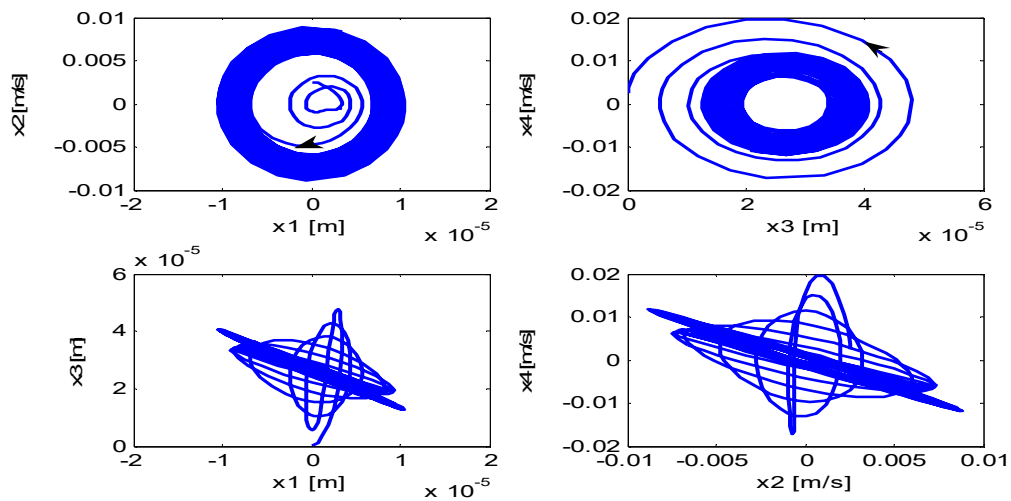


Fig. 10 The Phase plots of multibody turning model with $BC=80 \times 10^{-6}\text{m}$ when $\Omega=3000\text{rpm}$ and $w=0.5\text{mm}$. (The first row contains the phase plots of the tool and the workpiece respectively while the second row contains the plots of displacements which is a measure of cutting zone location. Instability is seen.)

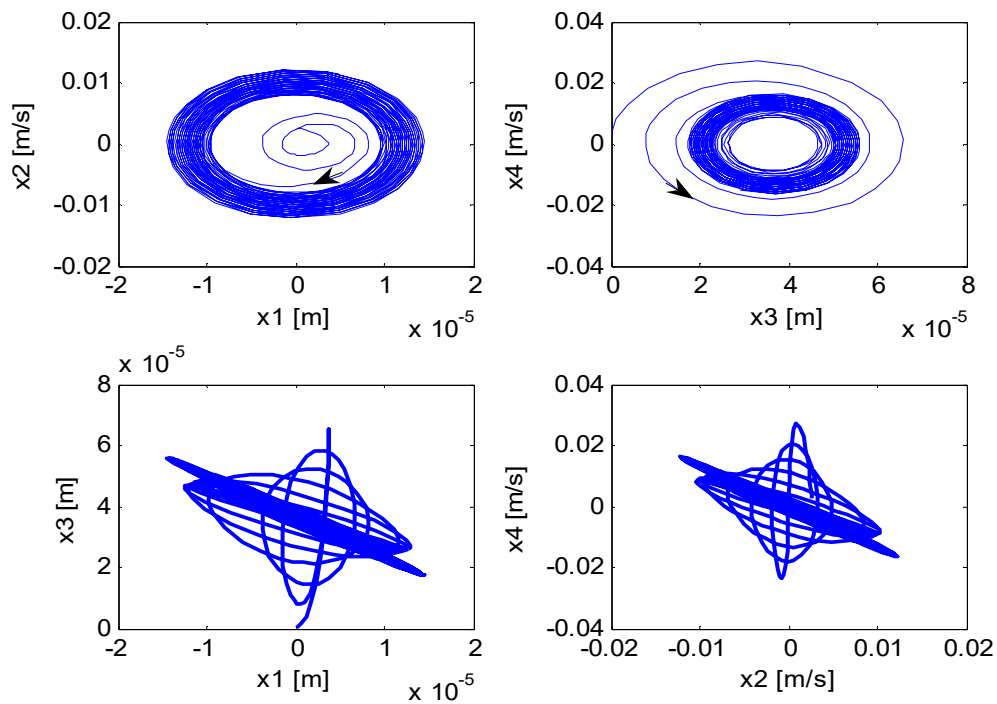


Fig. 11 The Phase plots of multibody turning model with $BC=110 \times 10^{-6}m$ when $\Omega=3000rpm$ and $w=0.5mm$. (The first row contains the phase plots of the tool and the workpiece respectively while the second row contains the plots of displacements which is a measure of cutting zone location. Instability is seen.)

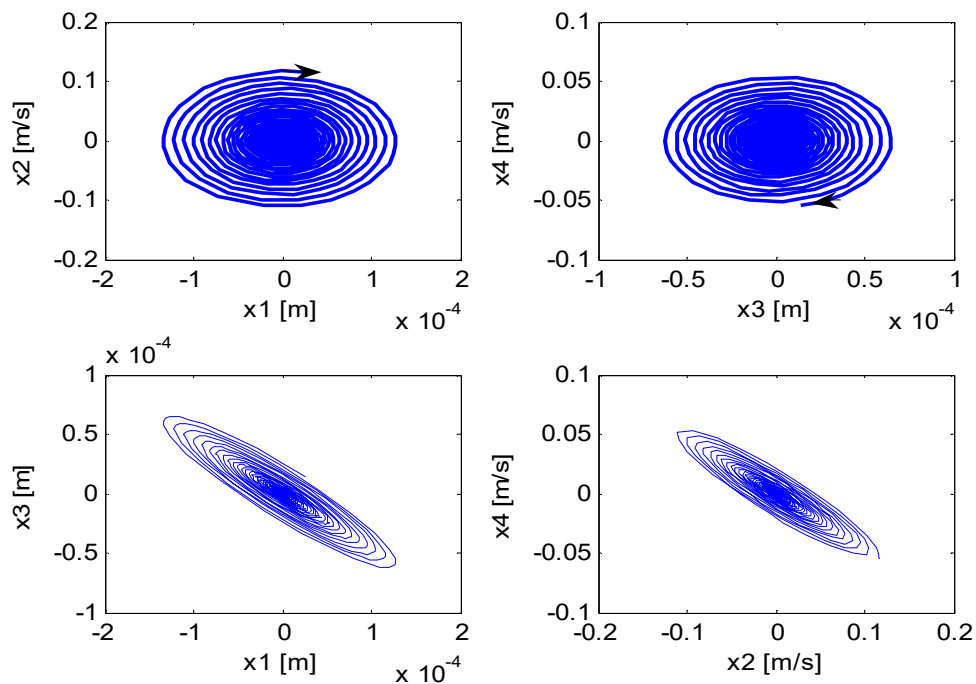


Fig. 12 The Phase plots of multibody turning model without BC when $\Omega=3000rpm$ and $w=1mm$. (The first row contains the phase plots of the tool and the workpiece respectively while the second row contains the plots of displacements and velocities which are measures of cutting zone motion. Instability is seen.)

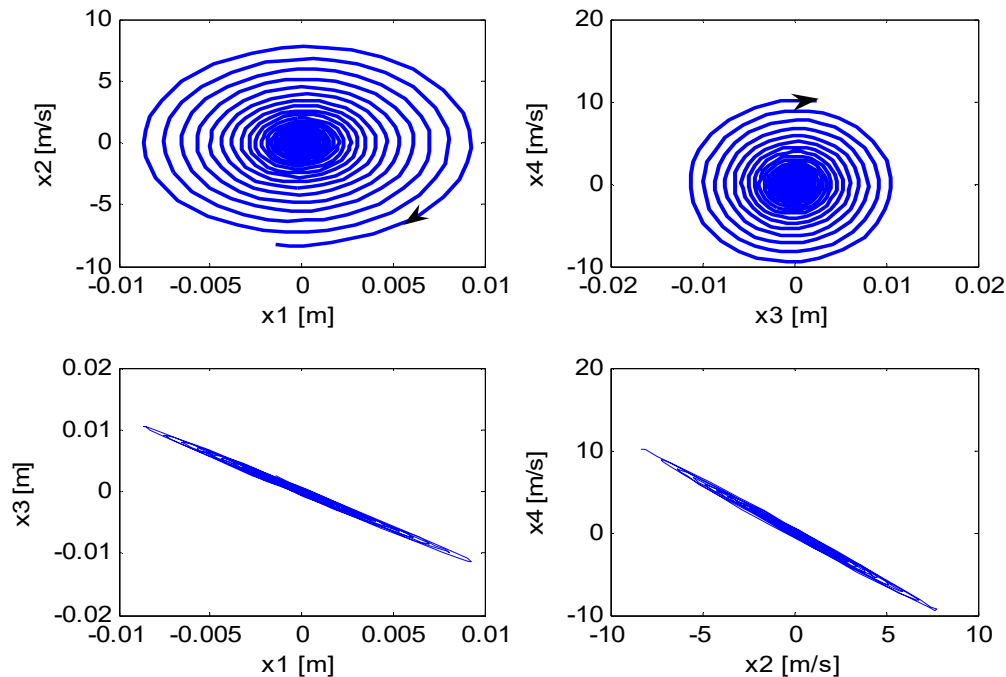


Fig. 13 The Phase plots of multibody turning model with $BC=80 \times 10^{-6}$ m when $\Omega=3000$ rpm and $w=1$ mm. (The first row contains the phase plots of the tool and the workpiece respectively while the second row contains the plots of displacements and velocities which are measures of cutting zone motion. Instability is seen.)

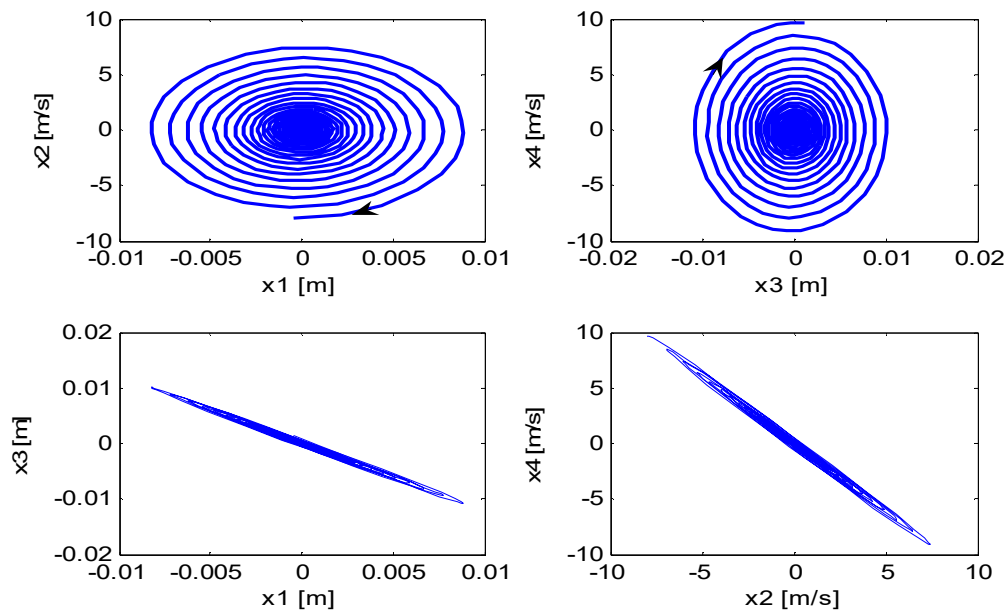


Fig. 14 The Phase plots of multibody turning model with $BC=110 \times 10^{-6}$ m when $\Omega=3000$ rpm and $w=1$ mm. (The first row contains the phase plots of the tool and the workpiece respectively while the second row contains the plots of displacements and velocities which are measures of cutting zone motion. Instability is seen.)

DISCUSSION

The above simulations are used to make deductions about the effects of bearing clearance on regenerative chatter stability of the derived multibody turning process model. Stability is deduced when a graphical solution from matlab dde23 solver converges with time to an attractor but instability is deduced when there is divergence instead. For example, turning regenerative chatter at the cutting conditions $[\Omega=3000$ rpm, $w=0.5$ mm] and $[\Omega=10000$ rpm, $w=0.5$ mm] are stable when there is no bearing clearance as seen in Table 2 but introduction of bearing clearance

destabilized the system. This is also reflected in the phase diagrams presented in Table 4 where the trajectories for the stable operations are attracted to the origin while the unstable ones diverge from the initial conditions. The rate of convergence/divergence to/from an attractor can be seen from a graphical solution and used to judge the location of a cutting condition relative to the boundary between the subdomains of stability and instability. For example, the solution in Figure 4 shows that at a cutting condition of $[\Omega=3000\text{rpm}$ and $w=0.5\text{mm}]$ with $BC=80 \times 10^{-6}\text{m}$, the system reluctantly diverges after recovery from the combined excitations from initial conditions and regenerative effects. This reluctance is an indication that the cutting condition is slightly beyond the boundary in the instability side [13]. The same goes for the same cutting conditions with $BC=110 \times 10^{-6}\text{m}$ as seen in Figure 5. The corresponding phase plots of the cutting condition $[\Omega=3000\text{rpm}$ and $w=0.5\text{mm}]$ with $BC=80 \times 10^{-6}\text{m}$ and $BC=110 \times 10^{-6}\text{m}$ shown respectively in Figures 10 and 11, reflect the slow rate of divergence. In Figures 7 to 8, it is seen that the cutting condition of $[\Omega=3000\text{rpm}$ and $w=1\text{mm}]$ with the $BCs=80 \times 10^{-6}\text{m}$ and $110 \times 10^{-6}\text{m}$ develops chatter fast. These means that they are markedly beyond the boundary in the instability side. This is seen in the corresponding phase diagrams found in Figures 13 – 14 where the phase trajectories steadily and rapidly diverge. It is known that the presence of bearing clearance in a machine could reduce the elastic stiffness of the whole machine system Peng et al. (2010). Natural frequencies are defined as $\omega_i = i\omega_1$ where $i=1, 2, 3, \dots$ and ω_1 is the fundamental natural frequency; for 1DOF system, $\omega_1 = \sqrt{k/m}$. Therefore, bearing clearance effect of reduced stiffness means a more flexible system that is more prone to unstable vibrations; when the fundamental or the dominant frequency of the machine system is high it becomes less likely to encounter a resonant excitation [7]. This is reflected in the simulation results summarized in Tables 2 - 4. The coupled tool and workpiece motions are stable at $[\Omega=3000\text{rpm}$, $w=0.5\text{mm}]$ and at $[\Omega=10000\text{rpm}$, $w=0.5\text{mm}]$ when there is no bearing clearance effect but recorded instability when bearing clearance of $60 \times 10^{-6}\text{m}$ is introduced at the same process parameter coordinates. In order to establish that more bearing clearance means more flexibility thus more instability, the system is re-simulated at $[\Omega=3000\text{rpm}$, $w=0.5\text{mm}]$ and $[\Omega=10000\text{rpm}$, $w=0.5\text{mm}]$ with much less bearing clearance of $5 \times 10^{-6}\text{m}$ as shown in Figures 15 to 17. It is seen that the system becomes more reluctant to destabilize as seen from the stable displacements and slightly unstable velocities because of reduced bearing clearance. These agree with results seen in Peng et al [13] for the milling process and more or less give validity to the results of model simulation obtained in the considered turning process with clearance influence.

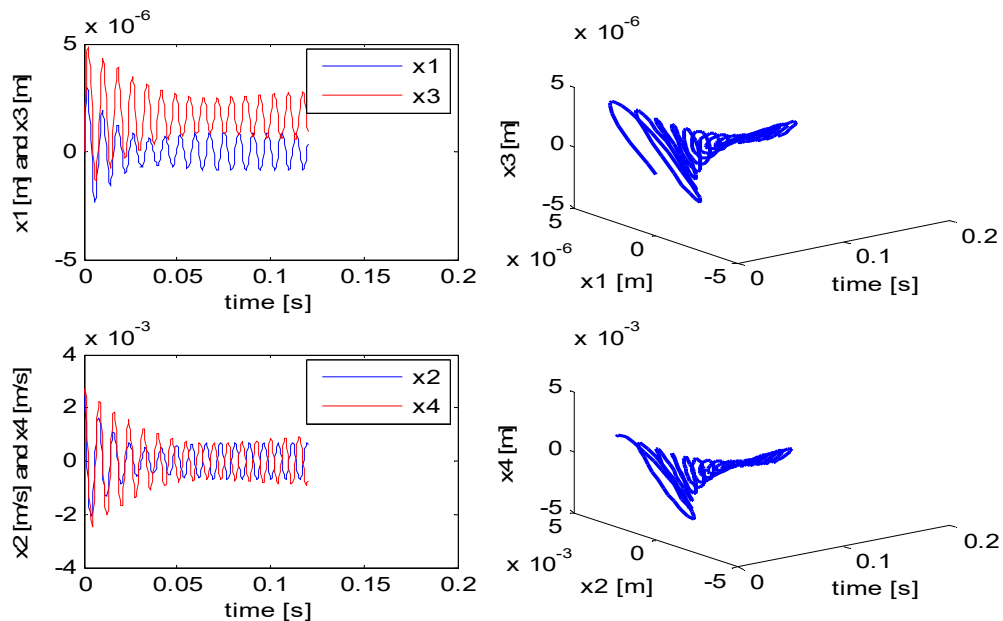


Fig. 15 The time histories of multibody turning model with $BC=5 \times 10^{-6}\text{m}$ when $\Omega=3000\text{rpm}$ and $w=0.5\text{mm}$. (Low rate of instability is seen).

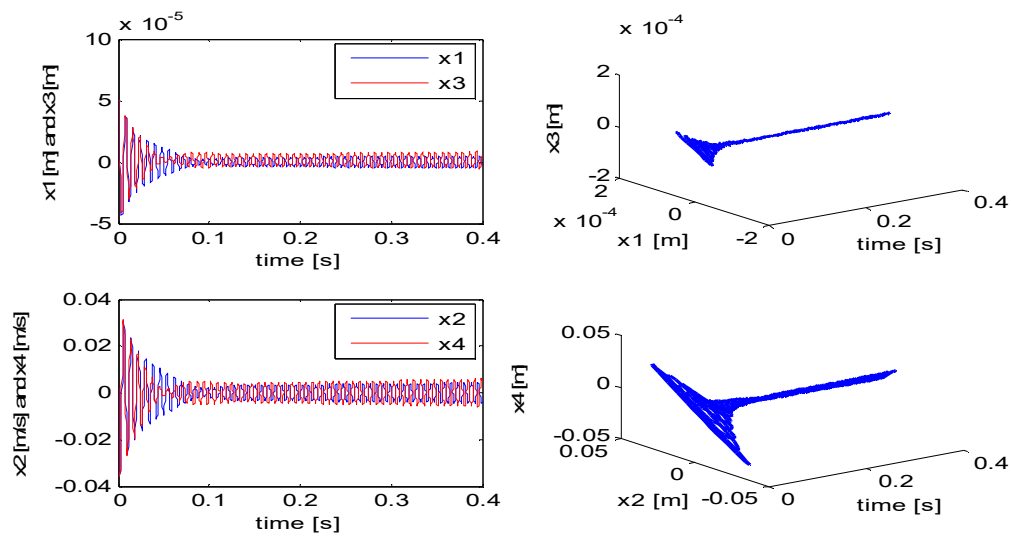


Fig. 16 The time histories of multibody turning model with $BC=5 \times 10^{-6}$ m when $\Omega=10000$ rpm and $w=0.5$ mm. (Low rate of instability is seen.)

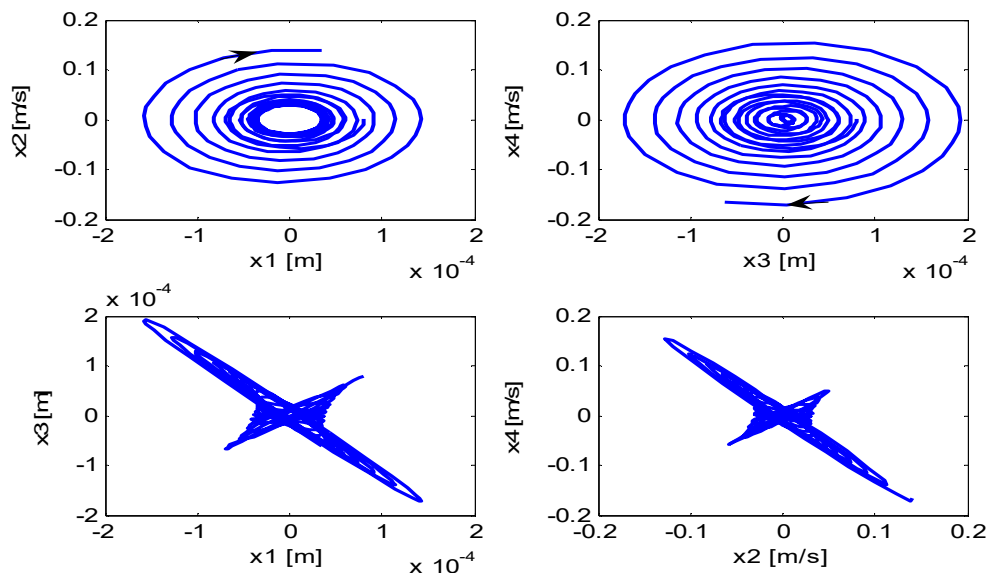


Fig. 17 The Phase plots of multibody turning model with $BC=5 \times 10^{-6}$ m when $\Omega=10000$ rpm and $w=0.5$ mm. (Slow rate of instability is seen.)

CONCLUSION

Chatter is the result of regenerative dynamic forces inbuilt in the machining process which can cause the system to be either stable or unstable depending on the parameters of the cutting operation and the dynamic features of the machine tool. In this paper, the vibration of a multibody turning process with and without bearing clearance has been considered and developed. Simulations in the forms of time histories and phase portraits were provided using a two-degree of freedom regenerative model. Turning regenerative chatter was stable at cutting conditions of $[\Omega=3000$ rpm, $w=0.5$ mm] and $[\Omega=10000$ rpm, $w=0.5$ mm], but instability results with the introduction of BC. It is established from the study that rate of convergence and divergence from an attractor indicates the domain of stability and instability. At cutting condition of $[\Omega=3000$ rpm and $w=0.5$ mm] with $BC=80 \times 10^{-6}$ m and $BC=110 \times 10^{-6}$ m the system diverges reluctantly, which indicates that cutting conditions are slightly beyond the boundary of instability. But at cutting condition $[\Omega=3000$ rpm and $w=1$ mm] with the BCs=0, 80×10^{-6} m and 110×10^{-6} m, process conditions were completely located in the region of instability, where chatter is markedly expedited. Hence the time histories and phase diagrams show rapid rate of divergence. The results of the simulation in terms of velocity/displacement histories and phase trajectories revealed that the bearing clearance effect reduces the elastic

stiffness of the machine system, thereby leading to system flexibility making the machine tool workpiece loop susceptible to unstable vibration. Employed for validation was historical data, which had been previously used to establish theoretically the BC effect in milling operation. The results of the validation at bearing clearance of 5×10^{-5} m revealed gradual paths to chatter instability, which more or less gave credence to the observed trend of divergence from the origin when BC is presence in the TDS.

REFERENCES

- [1]. J. Elias, V.N.N Namboothiri, Cross-recurrence plot quantification analysis of input and output signals for the detection of chatter in turning. *Nonlinear Dynamics* 76(2014) 255–261.
- [2]. U. Nair, B.M. Krishna, V.N.N. Namboothiri, V. Nampoori, Permutation entropy based real-time chatter detection using audio signal in turning process. *The International Journal of Advanced Manufacturing Technology* 46 (2010) 61-68.
- [3]. S. Stefania, K. Radoslav, M. Pollak, M. Kocisko, Research on impacts of mechanical vibrations on the production machine to its rate of change of technical state. *Advances in Mechanical Engineering* 8(7) (2016) 1–10.
- [4]. X. Song, X. Zhou, R. Chaudhari, S. P. Johnson, M. Kotzalas, Modeling and characterization of lathe spindle cutting patterns with crossed roller bearing installed. *International Journal of Mechanical Engineering and Robotics Research* 8(5) (2019) 660-666.
- [5]. C. Yuzhong, Y. Altintas, Modeling of spindle-bearing and machine tool systems for virtual simulation of milling operations. *International Journal of Machine Tools and Manufacture* 47(9) (2007) 1342-1350.
- [6]. G. Liu, J. Hong, W. Wenwu, Y. Sun, Investigation on the influence of interference fit on the static and dynamic characteristics of spindle system. *The International Journal of Advanced Manufacturing Technology* 99(2) (2018) 1953–1966.
- [7]. F.C. Moon, T. Kalmar-Nagy, Nonlinear models for complex dynamics in cutting materials. *Philosophical Transactions of the Royal Society a Mathematical Physical and Engineering Sciences* 359(1781) (2001) 695-711.
- [8]. M. Wiercigroch, E. Budak, (2001). Sources of nonlinearities, chatter generation and suppression in metal cutting. *Philosophical Transactions of the Royal Society of London. Series A*, 359(1781) (2001), 663-693.
- [9]. G. Stépán, Modelling nonlinear regenerative effects in metal cutting. *Philosophical Transactions of The Royal Society Biological Sciences* 359(1781) (2001) 739–757.
- [10]. C.G. Ozoegwu, Stabilizing wave attenuation effects in turning process. *Production and Manufacturing Research*, 2(1) (2014), 2–10.
- [11]. C.G. Ozoegwu, J.L. Chukwunke, I.P. Okokpujie, K.O. Babaremu, Stabilizing wave attenuation effects in high-speed metal cutting. In *Journal of Physics: Conference Series* 1378 (2019).
- [12]. P. Zmarzły, Influence of the internal clearance of ball bearings on the vibration level. 24th International Conference Engineering Mechanics 2018 Svatka, Czech Republic, May 14 –17, 2018 paper #97, pp. 961–964.
- [13]. Z.K. Peng, M.R. Jackson, L.Z. Guo, R.M. Parkin, G. Meng, Effects of bearing clearance on the chatter stability of milling process, *Nonlinear Analysis: Real World Applications* 11 (2010) 3577-3589.
- [14]. Vela-Martinez, J. C. Jauregui-Correa, E. Rubio-Cerda, G. Herrera-Ruiz, A. Lozano-Guzman, Analysis of compliance between the cutting tool and the workpiece on the stability of a turning process. *International Journal of Machine Tools & Manufacture* 48 (2008) 1054–1062.
- [15]. M. Wiercigroch, Modelling of dynamical systems with motion dependent discontinuities. *Chaos, Solitons & Fractals* 11 (2000) 2429-2442.